Factorization of partitions in two-dimensional lattices and complexity estimates

1998 J. Phys. A: Math. Gen. 31 9359

(http://iopscience.iop.org/0305-4470/31/47/001)

J. Phys. A: Math. Gen. **31** (1998) 9359–9376. Printed in the UK PII: S0305-4470(98)92619-1

Factorization of partitions in two-dimensional lattices and complexity estimates

Davide Bettati†, Mario Casartelli†‡, Paolo Celli and Luigi Malpeli†

† Dipartimento di Física dell'Università di Parma, I-43100 Parma, Italy

‡ Istituto Nazionale di Física della Materia, I-43100 Parma, Italy

Received 20 March 1998

Abstract. Connected partitions in two-dimensional lattices naturally arise in studying the cluster configurations of a large class of dynamical systems. We introduce a factorization into dichotomic factors allowing a meaningful implementation of the partition algebra. This factorization proves useful, in particular, in the reduction process between couples of partitions. The time-series approach to the complexity, based on the metric properties of the partition spaces, may consequently be extended from one- to two-dimensional processes. We check the efficiency of this formalism on the spin system simulated by the Q2R automaton.

1. The problem

The problem of factorizing finite measurable partitions into dichotomic partitions arises in the reduction process of rational partitions [1, 2]. In fact, the approach described in [2] is general, but its implementation fits only one-dimensional discrete configurations, i.e. strings. The procedure, implying a lot of interesting computational issues, is algorithmically very simple in that case, while its extension to two-dimensional spaces is a non-trivial one. Handling with partitions requires comparisons of boundaries of measurable sets, that are points in one dimension, and curves (possibly disconnected) in two, with a dramatic growth of operational complication. This has many facets: the very definition of 'elementary factors', the conversion of the partition algebra into computable procedures, and the correspondence of the introduced factorization to possible meaningful features of the objects under investigation.

After recalling basic definitions in section 2, we turn our attention to lattices, and in section 3 we give a complete solution to the problem within the class of two-dimensional *connected* partitions, by far the most important. The connection with complexity estimates is recalled in section 4, and in section 5 the efficiency of this approach and solution is checked on a concrete example, admitting easy generalizations.

2. Partitions, factors and reduction

For self-consistency, we recall some basic facts, notations and results about partitions, as given in [2].

In a probability space $(\boldsymbol{M}, \mathcal{M}, \mu)$, a partition α of $\boldsymbol{M}$, is an exhaustive, finite collection of disjoint measurable subsets, called 'atoms'. The set $\mathcal{Z}$ of all partitions is a metric space, with the distance

$$\rho(\alpha, \beta) = H(\alpha|\beta) + H(\beta|\alpha) \tag{1}$$

0305-4470/98/479359+18$19.50

where $H(\alpha|\beta)$ is the conditional Shannon entropy of α with respect to β. A partition α' is a *factor* of α if α refines α': therefore the atoms of α' are built up with atoms of α, and we write $\alpha' \leqslant \alpha$. This idea of a factor, introducing a partial order in $\mathcal{Z}$, is consistent with the following notion of a product: if α and β are partitions, their product $\gamma = \alpha \vee \beta$ (noted also as $\gamma = \alpha\beta$) is the coarsest partition among those refining both α and β. Atoms of γ consist of non-empty intersections of α and β atoms. The unit partition ν, having $\boldsymbol{M}$ as an atom, is a trivial factor for every partition. A factor is *dichotomic* when it has two atoms (a set and its complement in $\boldsymbol{M}$). It is 'prime' in the sense that it does not admit non-trivial subfactors. If α has n atoms, the family $D(\alpha)$ of all its dichotomic factors consists of $2^{n-1}-1$ elements. Since n may easily be 'large' (say, some thousand in concrete examples), the family $D(\alpha)$ cannot be handled directly. Moreover, $D(\alpha)$ generates α (i.e. $\vee\alpha_k = \alpha$ for $\alpha_k \in D(\alpha)$), but most of the factors are redundant for this purpose. Therefore, we wish to select an essentially restricted subclass $E(\alpha) \subseteq D(\alpha)$, whose elements shall be called 'elementary factors' of α. As discussed in [2], a criterion $\mathcal{P}$ extracting $E(\alpha)$ from $D(\alpha)$ must satisfy four conditions: (1) universality; (2) completeness; (3) self-compatibility and; (4) effectiveness. We shall briefly review these conditions later, referring to a defined class of elementary factors.

The main reason for introducing $E(\alpha)$ is the reduction of common factors between two partitions, in order to give evidence, as far as possible, as to their non-similar components. This is done by a 'reduction process' π working on couples of partitions:

$$(\alpha', \beta') = \pi(\alpha, \beta) \qquad \alpha' \leqslant \alpha,\ \beta' \leqslant \beta. \tag{2}$$

The procedure is the following. Suppose the elementary factors classes $E(\alpha)$ have been defined for every α. If $\sigma = \alpha \wedge \beta$ denotes the greatest common factor for a couple α and β, two classes $E(\alpha|\sigma)$ and $E(\beta|\sigma)$ are then introduced as those subcollections of $E(\alpha)$ and $E(\beta)$ which are 'prime' with σ;

$$\alpha_k \in E(\alpha|\sigma) \Rightarrow \alpha_k \in E(\alpha) \qquad \text{and} \qquad \alpha_k \wedge \sigma = \nu \tag{3}$$

and the same with β. The 'reduced' partitions $\alpha' \leqslant \alpha$ and $\beta' \leqslant \beta$ in (2) are then defined:

$$\begin{aligned} \alpha' &= \vee_k \alpha_k \qquad \alpha_k \in E(\alpha|\sigma) \\ \beta' &= \vee_j \beta_j \qquad \beta_j \in E(\beta|\sigma). \end{aligned} \tag{4}$$

The analogy with the cancellation of common factors in fractions motivates the term 'rational partitions' for reduced couples. However, since a uniquely defined factorization does not exist for partitions, the reduction π depends on the class $E(\alpha)$. Our problem is therefore to define $E(\alpha)$ explicitly, in the case of interest, with the purpose of optimizing the reduction in an easily computable way.

There always exists at least one solution to the problem of defining elementary factors: the class $S(\alpha)$ of 'simple' factors, each of them constituted by one single atom and its complement. However, even if conceptually simple, such a choice is non-practical for computer manipulations and (especially in more than one dimension) it is very severe with respect to the requirements of an effective reduction. We shall therefore introduce another factorization, easier to handle and more sensitive than $S(\alpha)$ to the structural features of the processes we are interested in.

3. The abstract lattice scheme

For definiteness, let $\boldsymbol{M}$ be a square lattice of $N \times N$ sites (or knots), K_r an r-values alphabet (typically, K_r is $K_2 \equiv \{0, 1\}$). A *configuration* is a function a: $\boldsymbol{M} \to K_r$, assigning a

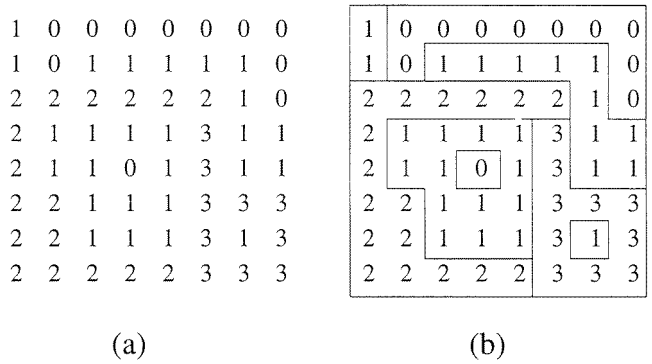

Figure 1. Example of clusters out of a configuration (*a*) and the related partition of the square (*b*).

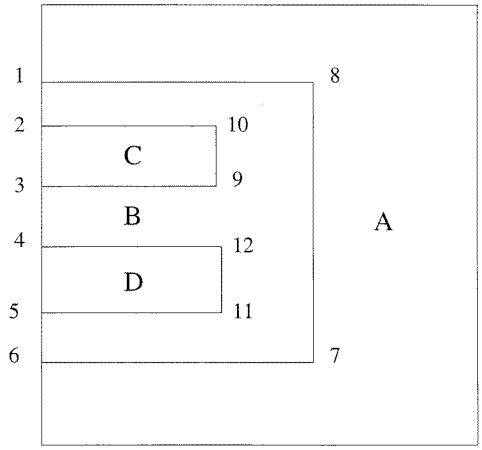

Figure 2. The external contour of atom B is through points 1-2-3-4-5-6-7-8-1; for C is 2-3-9-10-2; for D is 4-5-11-12-4 and for A is the whole frame.

symbol chosen in K_r to each site $x_{ij} \in \boldsymbol{M}$. The set $\mathcal{S}$ of all configurations has therefore cardinality $K_r^{N\times N}$.

Assuming, as usual, that the knots x_{ij} and x_{lk} are next neighbours when $|i-l|+|j-k| = 1$, knots may be grouped into a defined subset when they are homogeneous (same value in K_r) through paths connecting next neighbours. Such a procedure determines a partition of $\boldsymbol{M}$ (figure 1(*a*)), and it is consistent with a meaningful attitude in concrete problems, e.g. the characterization of a state of a spin system through the distribution of magnetization clusters. (For the two-dimensional Ising ferromagnet this approach goes back to Peierls [3], see also [4].) The procedure is also meaningful for those evolution rules which require 'differences' between next neighbours, i.e. when the dynamics depends on the cluster contours.

In fact, in order to identify atoms and clusters, we think about paths joining the centres of the adjacent 'plaquettes'. An atom corresponding to an isolated knot, for instance, is a square with one-step sides. Such contours determine a discretized partition of the dual $N \times N$ square, that for all practical purposes may be identified with the original partition of labelled knots in $\boldsymbol{M}$ (figure 1(*b*)). Thus, atoms are connected, but not simply connected in general, and their boundaries are (possibly multiple) paths. The number of included knots

divided by N^2 assigns a probability measure to each atom. Such a measure is the most natural to introduce in general, even if it is conceivable that other probabilities may better fit the features of particular processes. Generalizations to non-square lattices or planar graphs are also possible.

We have established a map $\Phi : \mathcal{S} \to \mathcal{Z}$, from the set of the lattice configurations into the space $\mathcal{Z}$ of partitions of the discrete $N \times N$ square. The following statements are straightforward.

S1. The map Φ is many-to-one, because we obtain the same partitions by permutation of symbols in K_r, and it is 'into' because there are partitions that do not correspond to any configuration. This is obvious, since disconnected partitions exist in $\mathcal{Z}$. Moreover, even considering connected partitions, the four-colours theorem says that there exist configurations corresponding to arbitrary partitions only if $r \geqslant 4$ in K_r.

S2. Every connected atom is identified by oriented boundaries. As usual, the positive orientation is assumed counterclockwise, leaving the 'internal' region on the left; an atom is bounded by one or more closed paths, but one and only one of them, the 'external' one, is positively oriented.

S3. Contours may partially overlap when they refer to different atoms (see also S5 below), but they cannot cross, since the crossing would imply a non-empty intersection (while atoms are always disjoint).

The following statements S4–S6 regard partitions when periodic boundary conditions are not used: indeed, in such a case, the frame (i.e. the border of the square) plays a special role.

S4. An external contour path may cross the frame only for an even number of times: indeed, every such intersection switches the internal and external domains of the atom, that would absurdly coincide after an odd number of switches.

S5. It is possible to modify the positive paths when they touch the frame, assuming as an 'external' contour of a given atom the whole piece of the frame between the first and the last intersection (obviously, this has some consequences only if there are more than four crossing points). Other atoms touching the frame between these extreme points must coherently be considered as internal to the given atom (see figure 2). This means that positive contours may partially overlap in the same direction along the frame, in opposite directions inside the square, and that the frame itself may be assumed as a contour. Without this assumption, the external domain of a positive path touching the frame four times or more would be disconnected. Another way of putting the same problem is as follows. If a path is not completely internal, then necessarily it has two and only two endpoints on the frame. Choosing a direction on this path means to define both the first and last endpoints and the internal domain. Such an internal domain is assumed to be the whole region contained by the path itself and the piece of frame between the last and first endpoints, independently of other atoms possibly contained there.

S6. There is, therefore, a one-to-one correspondence between atoms and positive contours; as to negative contours, they do not exist for simply connected atoms, otherwise they are (possibly multiple and disconnected) paths.

Statements S1–S6 would remain true even considering partitions with disconnected atoms, with obvious adaptations (e.g. positive contours would not be necessarily simple curves).

Finally, returning to connected partitions, we have the following.

S7. The internal and external domains to every positive contour are simply connected sets (note the role played by the assumption in S5 for non-periodical boundaries). Both of them are constituted by one atom or union of atoms, and therefore they define a dichotomic

factor of the original partition. This naturally introduces the factorization we are looking for.

Definition. The class $E(\alpha)$ of the *elementary factors* of α is constituted by partitions having as atoms the internal and external domains of the positive paths of α.

We must check the criterion $\mathcal{P}$ quoted above.

(1) Universality. This means that $E(\alpha)$ may be defined for every α. Obviously, there are no limits in introducing such a class of factors for every *connected* partition. For disconnected partitions (which we are not interested in) it all works the same, except for a pathological possibility, occurring when the disconnected parts of an atom A, say A' and A'', are in the relation $A' \subset B \subset A''$ with respect to another atom B. In this case, both the interior and exterior domains of a positive path intersect *the same* atom, and therefore do not define a factor of the primitive partition. Corrections to the definition are possible, of course, but we are not interested in such a generalization now.

(2) Completeness. This means that $E(\alpha)$ must generate α, i.e. $\vee_k \alpha_k = \alpha$ for $\alpha_k \in E(\alpha)$. Now, all contours have an interior, therefore they all occur as positive once: completeness follows.

(3) Self-compatibility. If $F(\alpha)$ is an *arbitrary* subcollection of $E(\alpha)$, define $\alpha' = \vee \alpha_k$ for $\alpha_k \in F(\alpha)$. From condition (1), $E(\alpha')$ is also well defined. Of course, since α' is generated by $F(\alpha)$, every $\alpha_k \in F(\alpha)$ is also in $D(\alpha')$. Self-compatibility means that $E(\alpha') \supseteq F(\alpha)$. Such a property is checked in this case by induction. Taking into account that the factors are labelled arbitrarily, let α_1, α_2 be two elementary α-factors. The partition $\alpha_{1,2} = \alpha_1 \vee \alpha_2$ has positive contours with a common piece, at most, because they cannot cross (see S3 above). As a consequence, the elementary factors of $\alpha_{1,2}$ are α_1 and α_2 selves. Now, by induction, let $\alpha_{1\ldots m} = \alpha_1 \vee, \ldots, \vee \alpha_m$. The product $\alpha_{1\ldots m} \vee \alpha_{m+1}$ does not break (for the same reasons) the positive paths already introduced; there is exactly one new path, the one defining the factor α_{m+1}. In other words, the elementary factors of $\alpha_{1\ldots m+1}$ are exactly $\alpha_1, \ldots, \alpha_{m+1}$. This shows that, if $F(\alpha) \subseteq E(\alpha)$ and $\alpha' = \vee_k \alpha_k$ for $\alpha_k \in F(\alpha)$, then $E(\alpha') = F(\alpha)$.

(4) Effectiveness. This requires that there are as many factors in $E(\alpha)$ as atoms in α (restriction of redundance). As already observed (statement S6), in our case there are as many positive contours as atoms. Note that (as for simple factors), $n - 1$ factors would be sufficient to generate α, but this further simplification is useless in practice.

This factorization generalizes the one used in [2] for one-dimensional partitions (in that case, left extremes of segments may be seen as 'external'). Hence, in principle, we have a suggestion for extensions to higher-dimensional lattices (even if the computational charge exceeds our present possibilities): it would be sufficient to collect the 'external' hypersurfaces of clusters.

The difference with respect to simple factors of $S(\alpha)$ is that, in this case, the reduction process requires the overlap of external contours only; taking into account that internal contours are external to some further atoms, the advantage is evident (also consider formula (3)). The example in figure 3 shows the efficiency of the reduction process in the two cases. We stress that the reduction does not consist in erasing the common lines, since the result of such a cancellation might be a non-partition. Moreover, in the algorithmical implementation of the process, all is made easier: stocking and handling of partitions, computation of distances, etc. Finally, we observe that our choice is, in a sense, the 'natural' one when configurations are produced through a rule involving next neighbours. Indeed, not only are the borders the sole sites that are active in the evolution (also simple

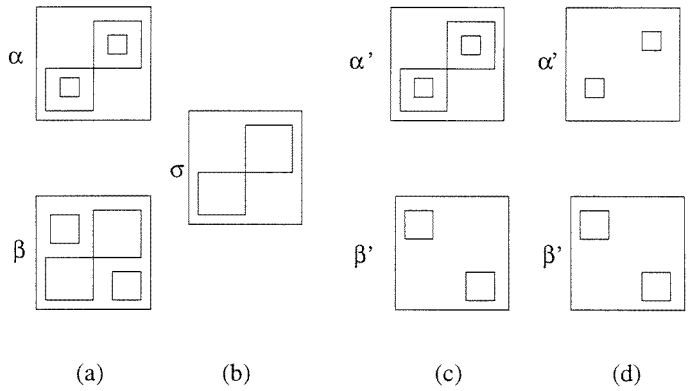

Figure 3. Two partitions α and β (a); their maximal common factor $\sigma = \alpha \vee \beta$ (b); the result of reduction using simple factors (c), or elementary factors described in the text (d).

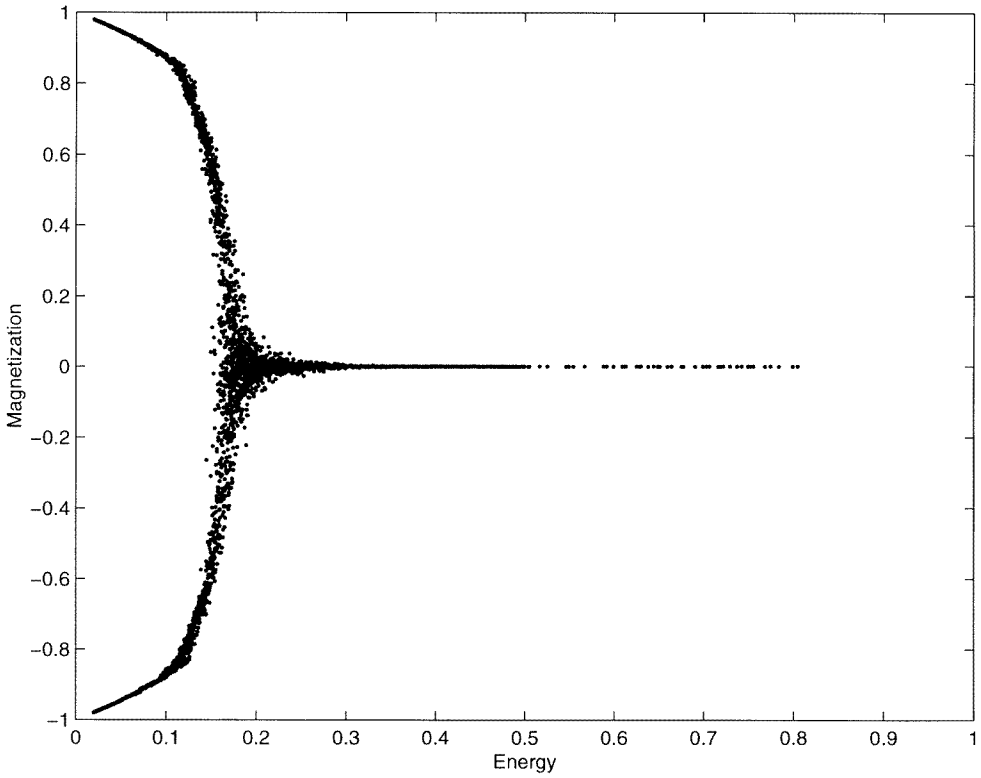

Figure 4. Mean magnetization versus energy E in the Q2R system, for several initial conditions.

factors reflect this feature) but, in addition, an external contour does not see what happens inside: to activate the reduction for the positive component of the contours, independently from the internal subconfigurations, seems therefore the proper choice.

In numerical simulations, one has: (1) to recognize and classify the boundaries of both partitions α and β (this is equivalent to defining elementary factors); (2) to build their

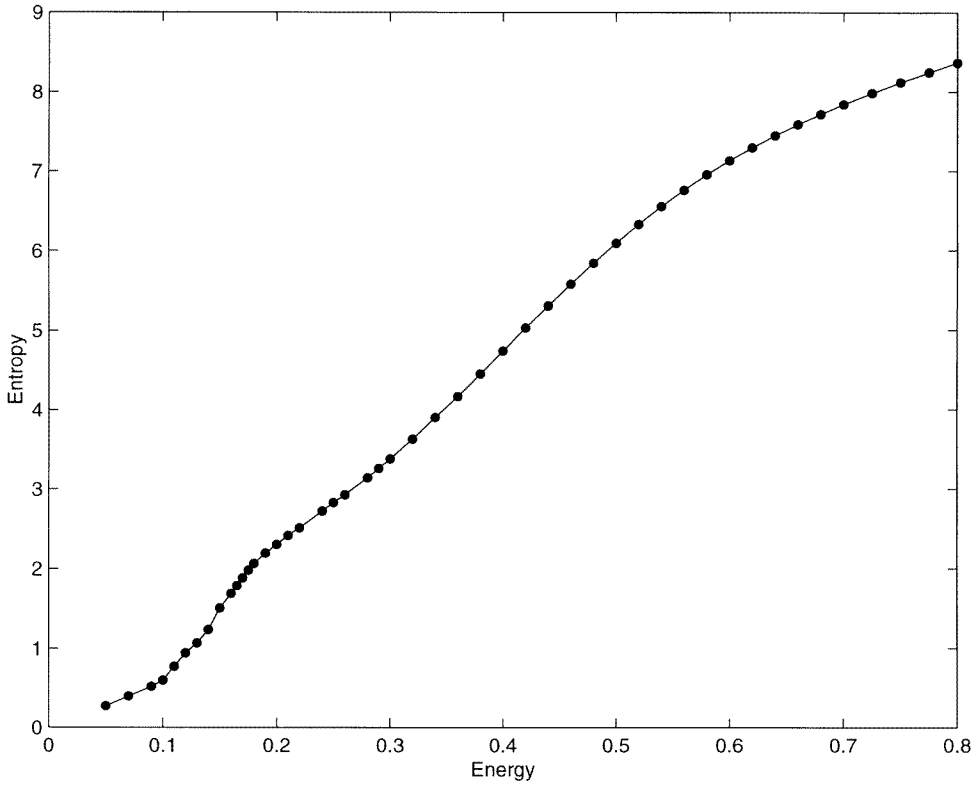

Figure 5. Time averages of entropy versus E for the Q2R system. The stabilization times used to get asymptotic values vary from 40 000 up to 450 000 steps.

greatest common factor $\sigma = \alpha \vee \beta$; (3) to eliminate those factors which are not prime with σ and; (4) to perform the product of the remaining factors, defining α' and β' as in (4). Moreover, in order to evaluate the distances before and after the reduction, one has to count the knots inside every atom for all partitions (reduced and not) and for their products. Indeed, instead of direct definition (1), it is convenient to use an equivalent formula where simple (non-conditional) Shannon entropy appears:

$$\rho(\alpha, \beta) = 2H(\alpha \vee \beta) - H(\alpha) - H(\beta). \tag{5}$$

As we shall see, in most cases the reduction process will refer to partitions obtained step-by-step from a sequence of evolving configurations. This means that whenever in the following we speak of reduction along a trajectory, the whole process is performed *at each step* (40 000 to 450 000 times).

One could object that the reduction loses its sense in the continuum limit, since the probability of exact overlapping of boundaries goes to 0. This is true, but (apart from the interest of intrinsically discrete processes) the meaning of this approach consists precisely in the fact that it simulates what happens, in general, treating the similarity of configurations *within a finite degree of precision*. To improve the precision means to increase N, in the model sketched above, without increasing the number of atoms.

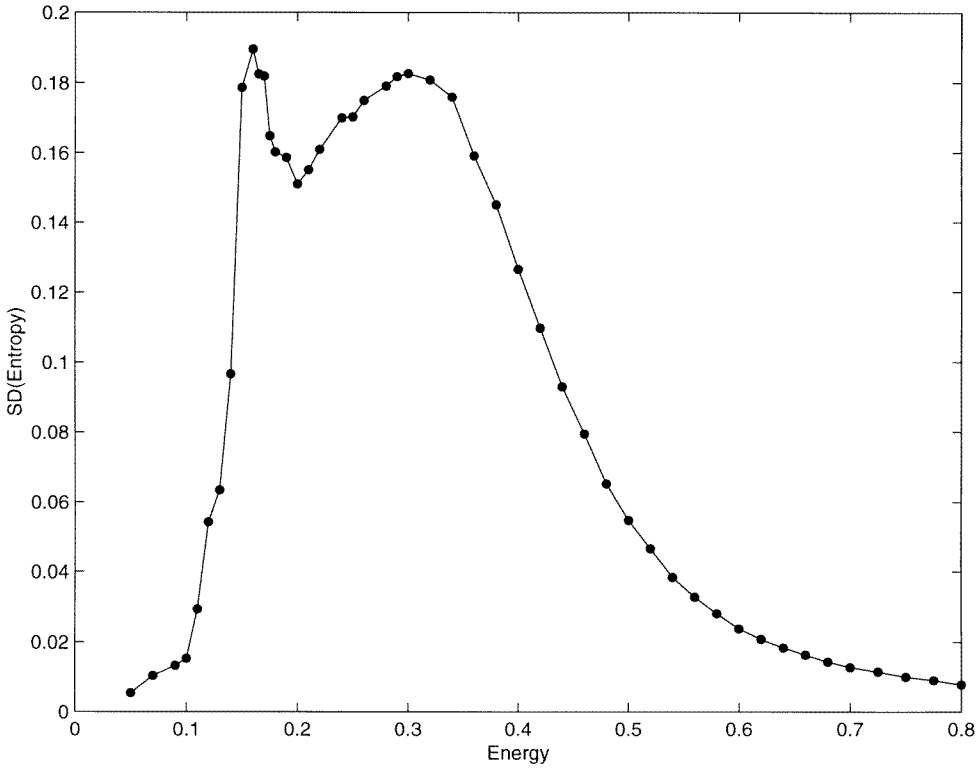

Figure 6. Standard deviations of the entropy (values along the orbits used to compute the time averages of figure 4) versus E.

4. Dynamics, partitions and complexity

Once the factorization and reduction formalism has been established, the approach to complexity is exactly the same as in the one-dimensional case: starting from an initial configuration $a(0)$, a dynamical system T in $\boldsymbol{M}$, defines the sequence $\{a(t)\}$ at discrete times $t = 0, 1, 2, 3, \ldots$, by $a(t) = Ta(t-1) = T^t a(0)$. The mapping $\Phi : \mathcal{S} \to \mathcal{Z}$ produces the corresponding sequence $\{a(t)\}$ of partitions by $\alpha(t) = \Phi(a(t))$. The implicit definition of the dynamical system $\tilde{T}$ in $\mathcal{Z}$ means, of course, $\Phi \circ T = \tilde{T} \circ \Phi$ and $\alpha(t) = \tilde{T}\alpha(t-1) = \tilde{T}^t\alpha(0)$.

The sequence $\{\alpha(t)\}$ is the actual object of our analysis. Several time series may be calculated on it. We shall consider for instance (but not exclusively) the following quantities.

- The entropy of the partitions, $H(t) = H(\alpha(t))$ which measures the complicacy of every single partition taking into account the distribution of the cluster measures, not their shapes.
- The entropy $S(t) = H(\sigma(t))$ of the intersection $\sigma(t) = \alpha(t) \vee \alpha(t+1)$ between two next partitions which gives the degree of their overlapping.
- The distance $d(t) = \rho(\alpha(t), \alpha(t+1))$ between the two next partitions which measures how much they distinguish from each other, and in this case relative shapes are relevant.
- The distance $d_r(t) = \rho(\alpha'(t), \alpha'(t+1))$ between the *reduced* partitions; possibly, the previous quantity is amplified by the erasure of common factors. The very definition of factors is therefore important here.
- The amplification factor, $A(t) = d_r(t)/d(t)$ which measures the relevance of the

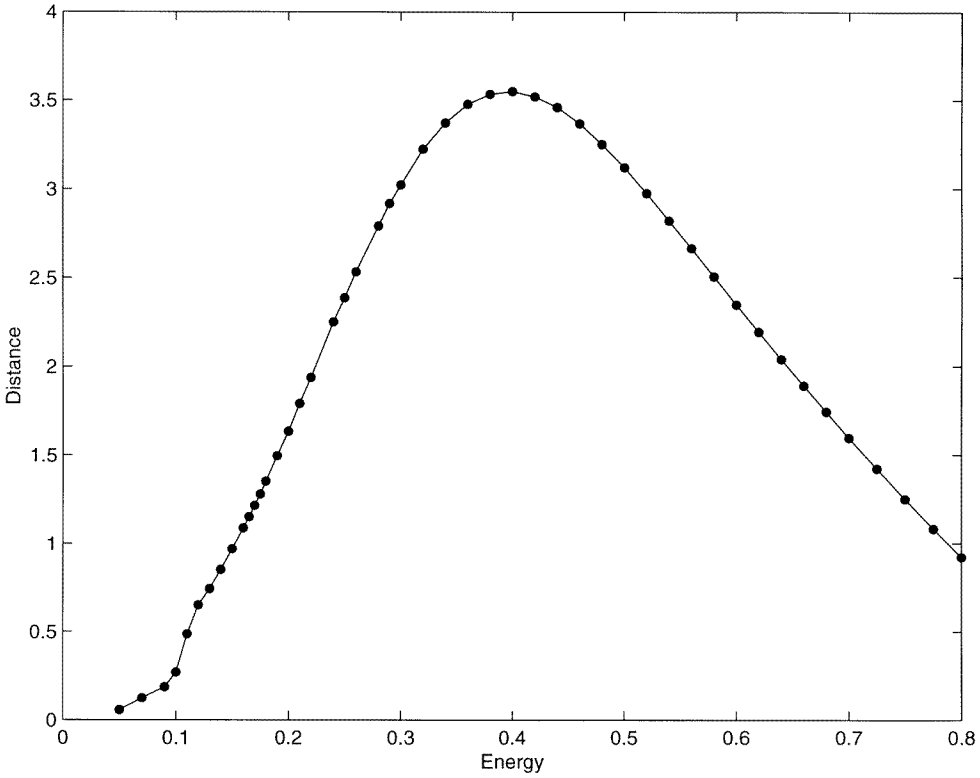

Figure 7. Time averages of distance between next configurations versus E.

reduction process.

There are several meaningful combinations of these quantities. For instance, the bare entropy may be used to weight other observables, such as $S(t)$. The coherence and reliability of the results may be tested by varying the parameters in numerical experiments, e.g. by computing time series with time intervals longer than one step, or by examining the dependence on initial conditions and the length of transient regimes, etc. Experience on one-dimensional processes [2] tells us that, through usual statistical operations (time averages, standard deviation, Fourier analysis etc), the whole set of observables can provide a rich pattern of information on the process, even if a single one of them may be misleading in some circumstances.

5. The microcanonical spin automaton

This apparatus has been tested, as in the one-dimensional case, mainly on cellular automata, whose configuration spaces fit the features sketched above. We shall report some results of numerical simulations on the Q2R automaton, a well known model simulating a microcanonical spin system. These experiments are intended as a check of the reliability of the partition formalism, not as an exhaustive study on spin systems. In this spirit, we omit the results involving the Fourier analysis of the time series; the onset of correlated complexity on spatial and temporal bases requires a discussion beyond the limits of a simple check. For instance, we should introduce comparisons and references to the so-called self-

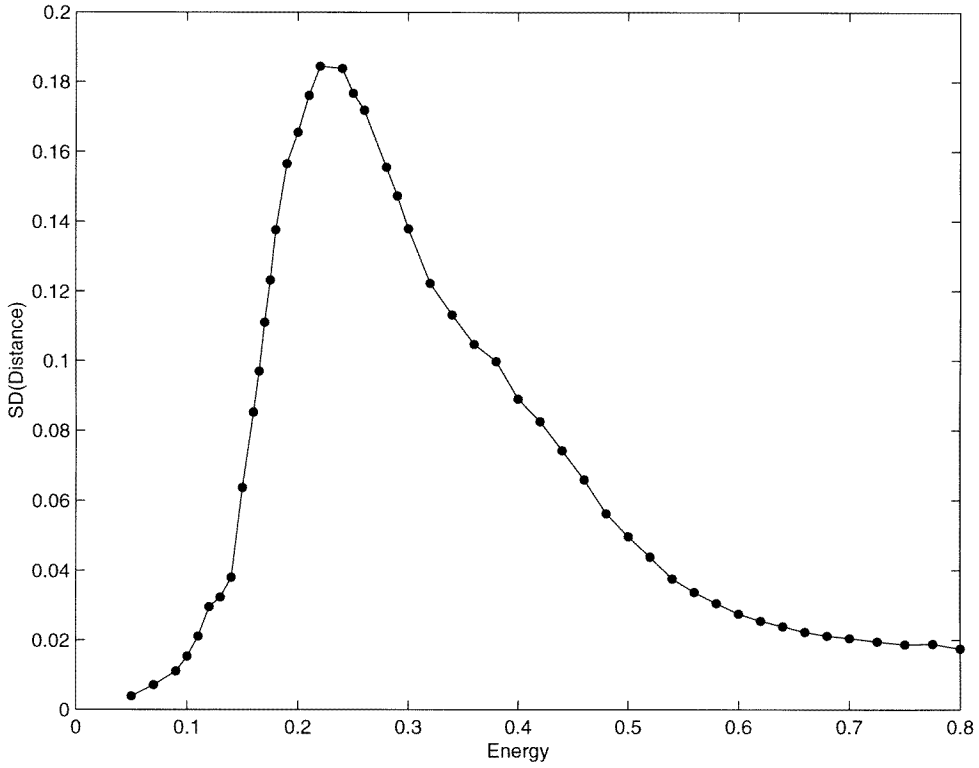

Figure 8. Standard deviations of the distances along the orbits versus E.

organized criticality. All this will be presented elsewhere.

For a review on complexity versus phase transitions and underlying problems, see [5–11] and references therein. For general information on the Q2R automaton, see [12–14]. We only recall that the deterministic rule, which applies separately to the even and odd sublattices, forces a knot to flip (exchanging values 1 or 0 for spin up or down) if and only if the sum of the nearest neighbours is 2. This means 0 transfer of energy. Consequently, the energy E defined by

$$E = \frac{1}{4N^2} \sum_{i,j} \sum_{\langle l,k \rangle} |x_{ij} - x_{lk}| \tag{6}$$

where $\langle l, k \rangle$ are the first neighbours to i, j, is a constant of motion. The magnetization is

$$M = \frac{2}{N^2} \sum_{i,j} x_{ij} - 1. \tag{7}$$

It is well known that, because of the finite size of the lattice, a proper critical energy E^c is not defined, and nevertheless it is possible to observe a sort of phase transition in a band around a value E^0, empirically defined by the flexus in the magnetization curve going from definitely positive or negative mean values, to the mean value 0. In our units, where the maximum of energy is 1, this value E^0 is 0.175 ± 0.005, the transition band ranges from 0.11 to 0.25 (figure 4). It is also known that for an infinite lattice the correlation length diverges at the transition, with the onset of a fractal structure of clusters. This behaviour (within the finite-size approximation) may be observed in the band, and may also be partially checked

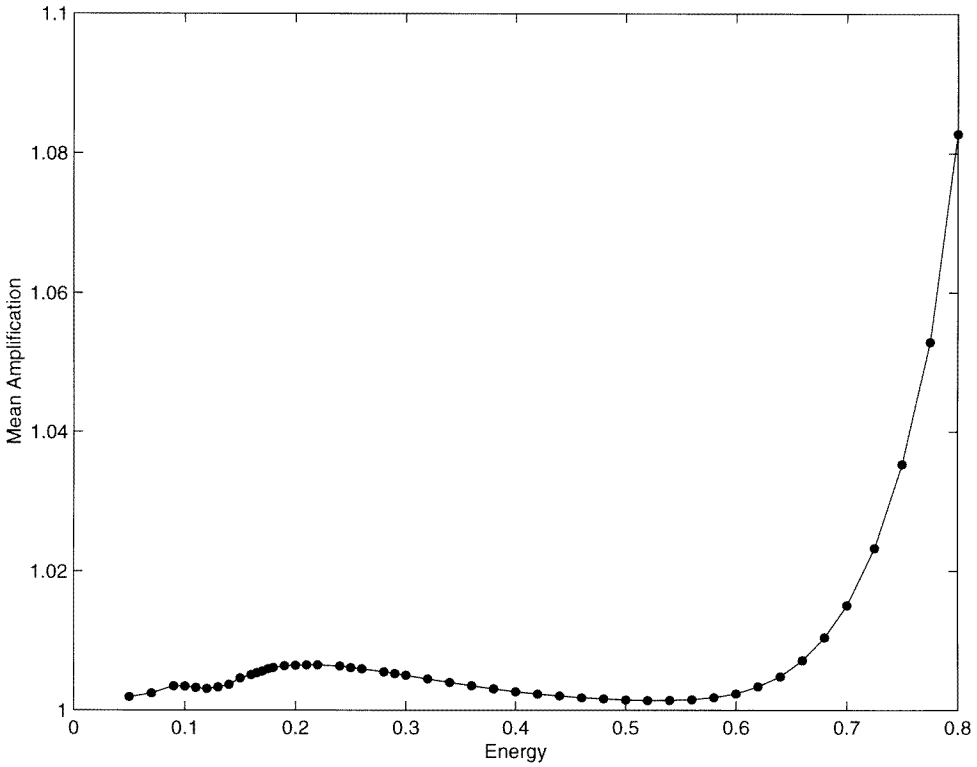

Figure 9. Mean value of the amplification factor versus E.

through visual inspection; the configuration patterns are well known and easily available (see e.g. [7, 14]).

We recall that the maximum of energy ($E = 1$) corresponds to a regular chessboard, therefore simulations lose their meaning in this limit, even the onset of 'chess-like' antiferromagnetic domains could be an interesting point in further studies. In order to avoid misinterpretations, we shall run experiments up to $E = 0.80$.

Below or above the transition band, ordered and chaotic behaviours are expected, respectively. At low energy, order means dependence on the initial conditions, and the presence of periodical configurations. This behaviour has indeed been found, but in the following diagrams we do not show a large sample of results for $E < 0.1$, where at every energy one should consider a whole (and, for actual purposes, non-interesting) distribution depending on the initial values. As for chaotic behaviour, for a deterministic finite (and therefore periodic) cellular automaton this notion requires some clarification. It could be intended, for instance, as 'damage spreading', referring to the growth of a tiny perturbation. Moreover, in general, it could mean that, for all relevant observables and for evolution times sufficient to obtain stabilized averages, there is a (more or less perfect) coincidence with the results given by a random automaton (i.e. an automaton whose sites evolve independently from one another according to a probabilistic law). This is what we mean by chaotic. In particular, looking at configurations at high energy, chaos implies the vanishing of large structures and the local instability of fine structures.

Numerical simulations have been performed on a Silicon Graphics SG1 Indigo2–

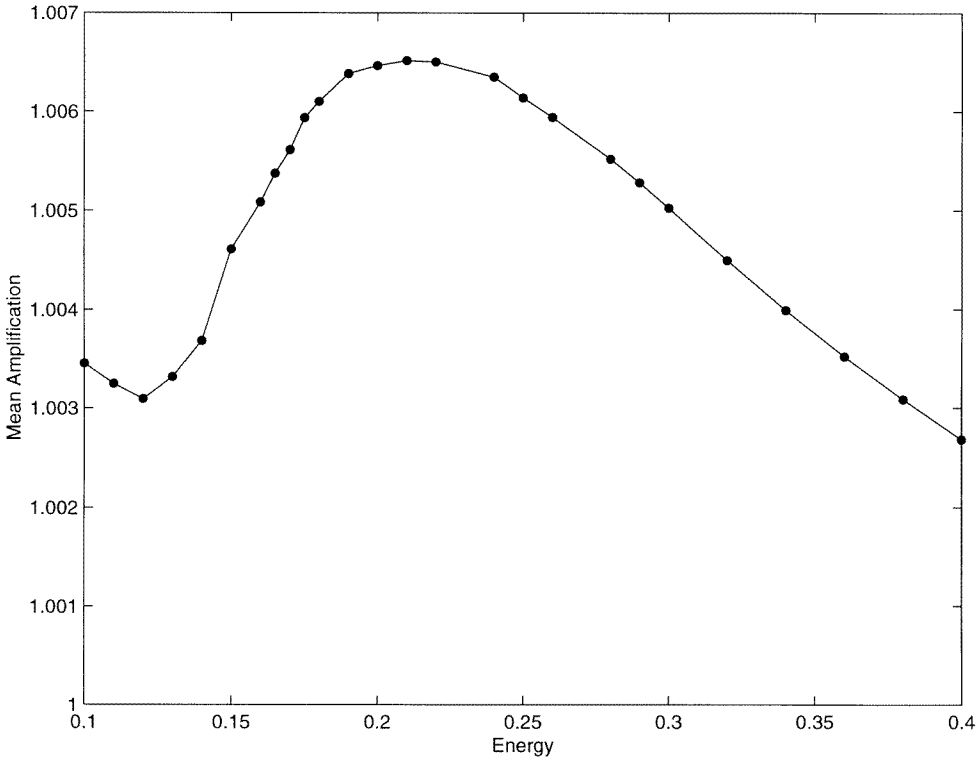

Figure 10. Zoom of the previous figure.

R4400 XL, and on a Digital AXP 600 5/266. The size of the lattice in most experiments has been $N = 100$. To get asymptotic (i.e. well stabilized) values in the time averages and standard deviations along the trajectories, orbits have been computed up to a maximum time t_{max} depending on the initial conditions, since the transition values of the energy require longer times. In the following, reporting time averages, we omit to note t_{max} explicitly. Some further information is therefore necessary.

• Out of the transition band, a typical value is $t_{max} = 40\,000$ steps, large enough to give an excellent stabilization, but in the purely chaotic situation even $t_{max} = 8000$ would have been sufficient. Stabilization means that longer runs do not improve anything, i.e. error bars would remain within the circles of the figures we shall present. Moreover, the results would be qualitatively clear even with half-time.

• In the transition band around E^0, there occur fluctuations on much longer timescales. Standard deviations are particularly sensitive to such fluctuations. We get a good stabilization in the previous sense using t_{max} from 150 00 up to 450 000 steps.

• The possibility of further fluctuations on a much greater timescale cannot be excluded. However, by observing the evolution of our diagrams, we see that the evidence of our conclusions does not weaken with time. Therefore, we may have some confidence that they are reliable, independently of the possibility of changing the order of magnitude in the computation runs.

• Obviously, the occurrence of these fluctuations is in itself a complexity indicator, confirming the expected difference with respect to a purely chaotic behaviour.

Initial configurations have been chosen through a random number generator, but, in order

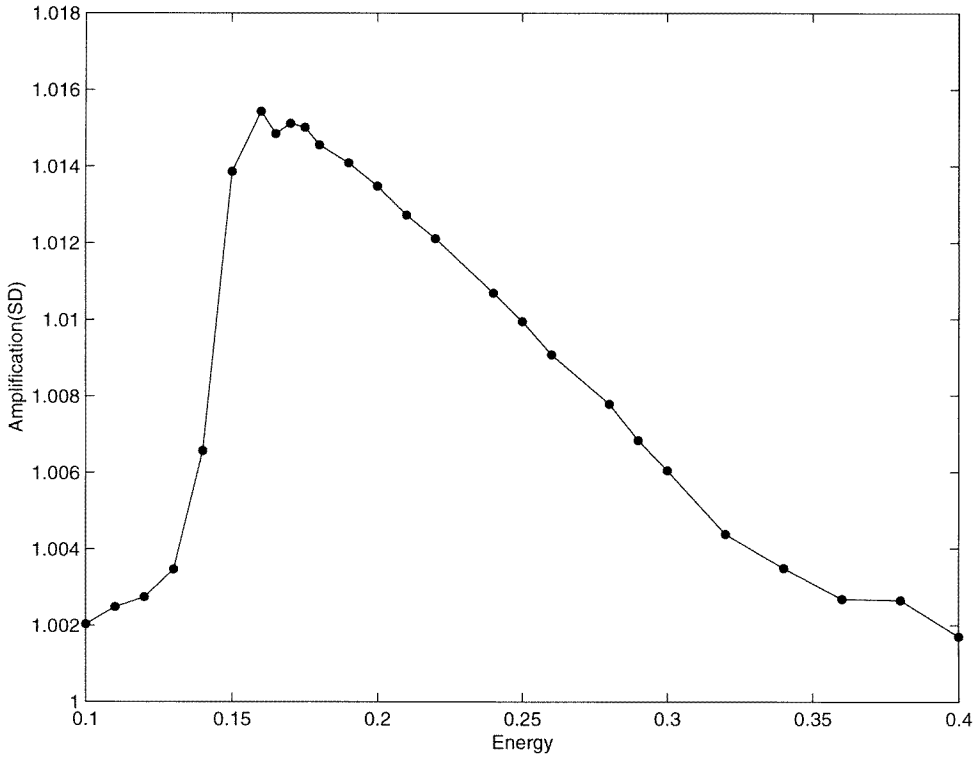

Figure 11. Zoom of standard deviations along the orbits of the amplification factor.

to shorten the stabilization time, a transient 'free' evolution, before starting the averaging on various observables, is very useful. This transient is also much longer, as expected, in the transition band. Indeed, a random generator does not spontaneously produce fractal structures, as those slowly shaped by dynamics. For uniformity the same long transient of 100 000 steps has been used, even if unnecessary.

Figure 5 shows the time-averaged entropy $\langle H(t)\rangle$, as a function of the energy E. After a quasilinear growth for $E < 0.6$, it begins to slow down (remember that there is a maximum, $H = 2\log N$, corresponding to the chessboard). A small bump around the transition could be noticed, but the general behaviour is very regular.

The standard deviation of the same quantity along the orbit (figure 6) is more interesting: there is a first maximum, a very neat peak, coinciding with the transition, and another smoother maximum after the exit of the transition band. Since the standard deviation is an index of time fluctuations, the locations of these maxima strongly support the idea of a particularly complex behaviour in the band, while the distinction between them, likely related to the breakdowns of magnetization and fractality, respectively, is not clear to us in its dynamical details. As to the decreasing behaviour with the onset of chaoticity, it may be easily interpreted with reference to the smaller and smaller size of the evolving atoms, providing stabilization in time, i.e. only small fluctuations of entropy.

Figures 7 and 8 show averaged distances $\langle d\rangle$ and their standard deviations $SD(d)$, i.e. the diagrams for distances corresponding to the two previous ones. Distances grow linearly, in figure 7, from the ordered domain, where the magnetization is definitely non-zero, up to the transition band. This simply says that the relative dissimilitude between configurations

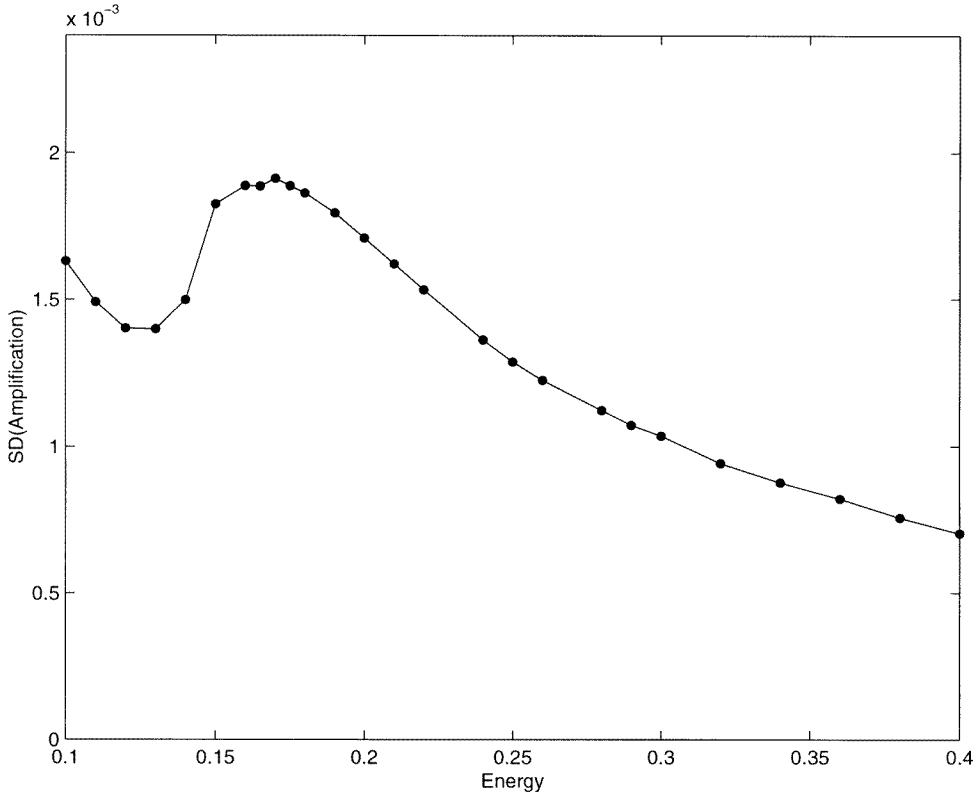

Figure 12. Zoom of the amplification (ratio) between standard deviations referring to reduced and non-reduced distances (the denominator is figure 7).

increases with energy. But, since the energy depends on the length of the cluster boundaries, it is a non-trivial information that such a nonlinear functional in $\mathcal{Z}$ as (1), based on the atom-intersections areas, depends *linearly* on this length in the time average. Hereafter the growth slows down and the maximum is reached just *after* the breakdown of the fractal structure. The final decrease may be ascribed to the fragmentation into smaller and smaller atoms: this fragmentation indeed makes more and more similar the configurations, notwithstanding their growing mobility.

In figure 8, the peak is nearby the end of the strictly linear growth of figure 7, within the transition band but after the empirical value E^0. One can read here that, up to the establishment of the fractal structure, the fluctuations of similarity between next configurations also increase very rapidly. Once again, the subsequent decrease can be interpreted as a stabilization effect due to the chaos itself. Therefore, the shift of the maximum with respect to E^0 is likely due to the balance between fluctuations in time (remember that the mean distances are still growing here) and the fragmentation of cluster in the fractal regime, the process which contributes to the stability in the time behaviour.

We do not report diagrams for the reduced distances, qualitatively identical to the previous ones. However, the reduction process carries relevant information on the cluster dynamics. Consider for instance, in figure 9, the amplification in the mean:

$$\bar{A} = \langle d_r \rangle / \langle d \rangle \tag{8}$$

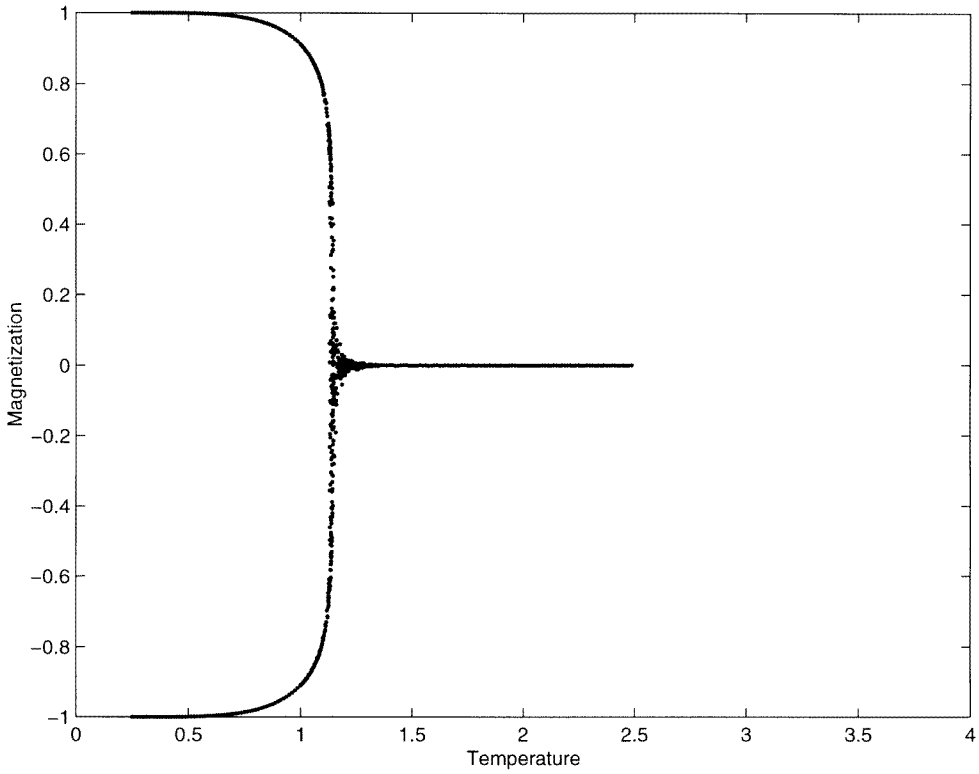

Figure 13. Mean magnetization versus temperature in the canonical system, to be compared with figure 4.

i.e. the ratio between averaged distances (reduced over non-reduced ones). Even if the reduction is very small, we can clearly distinguish a first maximum in coincidence, once again, with the transition, just after E^0. Then, up to the establishment of the full chaotic regime, there is a slow decrease, and finally a new rapid increase. This last growth phenomenon, even if impressive, is in a sense trivial, since it may be related to the abundance of small contours, the easiest ones to be reduced. In contrast, the first part of the diagram, shown as a zoom in figure 10, is not obvious: starting from the ordered regime ($E = 0.1$), the first light decrease means that the mobility of contours grows, at the beginning, in such a way to lower the reduction probability. But almost immediately the balance is inverted. Evidently, the gain due to the reduction can grow only if configurations are not too poor. Up to the birth of large clusters, the growth of the amplification factor means that the balance between contour mobility and richness of possible configurations is such that the contour overlaps increase. The maximum is again coherent with the full establishment of the transition, just after E^0. Then there is another inversion: the clusters mobility and the relative abundance of long contours progressively restrain the reduction, up to the disintegration of large clusters. What happens there is clear from the previous figure. Note that the same pattern holds for the time average of the amplification factor, producing an almost identical figure which we do not report.

Even if the numerical range is narrow, the same peak appears in figure 11 (we directly

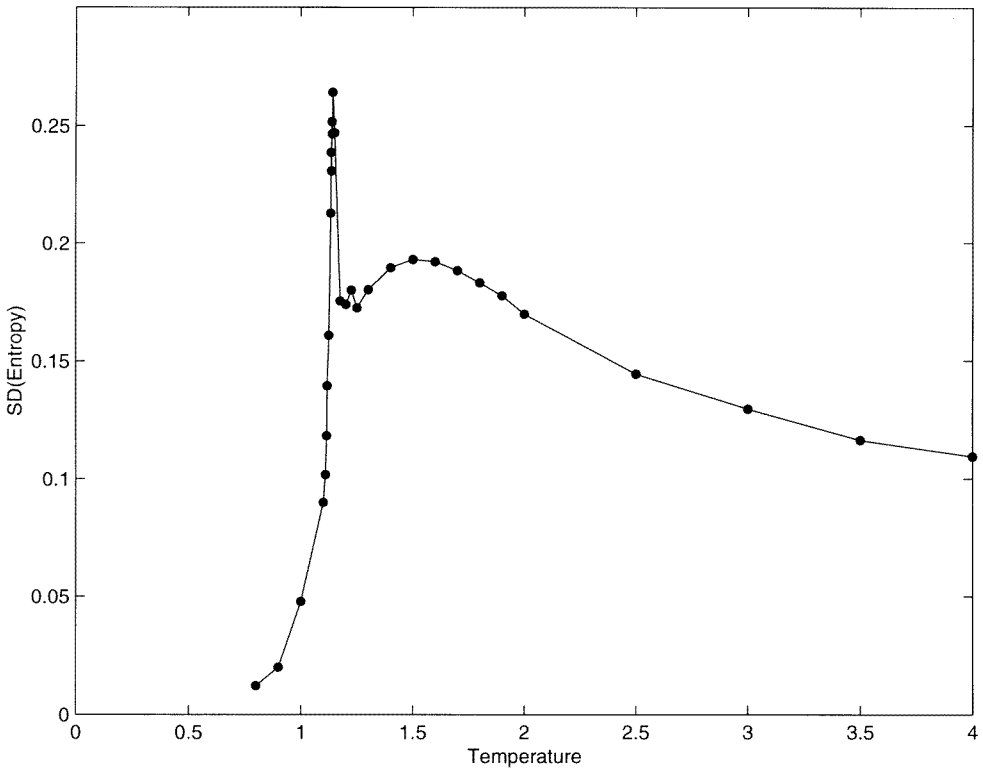

Figure 14. Standard deviations for the entropy values along the orbits versus temperature for the 'canonical' system (to be compared with figure 5).

zoom in on the interesting energy range). It gives the quantity

$$SD(A(t)) \equiv SD(d_r(t)/d(t)) \tag{9}$$

i.e. the standard deviation of the amplification factor along the orbit. This means that, coherently with the reduction in the mean, during the fractal phase of configurations the reduction process also undergoes a maximum for fluctuations in time. In terms of cluster behaviour, we observe that, according to the rule, only the contours may contribute to dynamics. But in the presence of big clusters, small fragments may sever, and such fragments of one or two sites do not evolve in the next step. Therefore the corresponding atoms are erased by reduction. The intermittency of such a reduction mechanism is responsible for large time fluctuations of the amplification factor.

It is also interesting to observe in figure 12 the diagram of

$$SD(d_r(t))/SD(d(t)) \tag{10}$$

i.e. the ratio of the standard deviations of distances (reduced over the non-reduced one). Ratio (10) is not, as the previous one, a measure for the instability of the amplification factor, but as the amplification factor of the time instability of distances. The fact that this quantity is slightly greater than 1 for all energies simply means that 'useless' reduced factors work to stabilize the configurations, as expected; but we see in addition that the maximum of this effect is attained within the transition, and the coincidence of the peak with E^0 is striking.

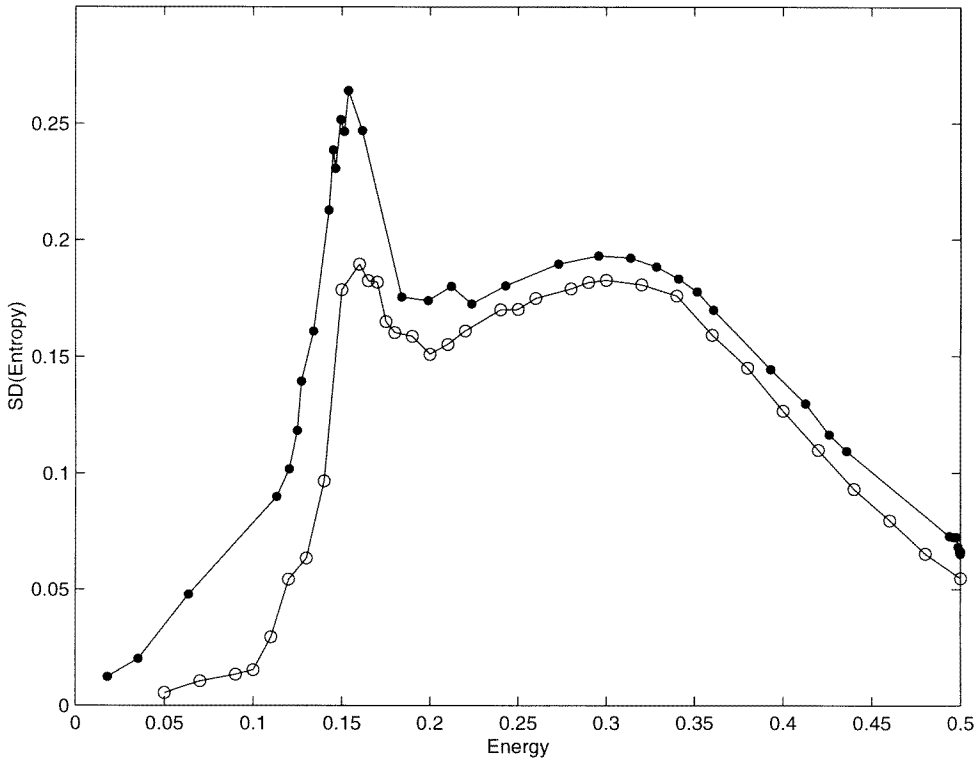

Figure 15. Standard deviations of entropies of microcanonical (empty circles) and canonical (full circles) systems versus energy.

It is a truism that the features listed above depend on the dynamics, but a doubt naturally arises: they could strictly depend on the Q2R evolution rule, having nothing to do with the transition from order to disorder in magnetic lattices. Therefore the experiments have been repeated for another automaton, using the Metropolis evolution rule, i.e. a probabilistic dynamics providing a description of the spin lattice in the canonical formalism (see e.g. [14]). As in the previous case, a single evolution step consists of a complete updating of the lattice. The transition band (around a pseudo-critical temperature $T^0 = 1.125$) is sharper than in the Q2R case (see figure 13). Also, the transient evolution necessary to reach a steady dynamics is drastically shortened.

It is noteworthy that, at least qualitatively, nothing changes in most of the diagrams we have presented (apart from the obvious substitution of energy with temperature), and the clearness of indications is generally improved. See for instance in figure 14, corresponding to figure 6, the diagram for the entropy standard deviation. The two-maxima structure is very well preserved, and the coincidence of the first peak with T^0 is particularly impressive (compare with figure 13). A further illustration of the qualitative overlap of the results may be seen by displaying the entropy of figure 14 as a function of the mean energy, instead of temperature, in such a way to have a direct comparison between the two systems; this appears in figure 15.

This answers the critic: the robustness of the results with respect to deeply different evolution rules seems to indicate that the description of the transition phenomenon is accurate and reliable.

Of course, there are also some differences: the new evolution rule does not only involve the contours. This has a certain influence on the reduction process, especially at low temperature (with respect to the previous low-energy case). Small atoms on a uniform background, corresponding to one or to two knots, tend to be stable in the Q2R evolution, instable with the new rule. Therefore they are reduced in the former case but not in the latter. For temperatures below T^0 this implies some minor modifications of diagrams corresponding to those in figures 9 and 10. On the other hand, this confirms the sensitivity of our indicators to the details of the shape dynamics.

Once again, as noticed for one-dimensional systems in [2], spatial 'difficulty in description' (fractality) and dynamical instability seem structurally related, as confirmed by extremely long fluctuations during the transition (the appearance of $1/f$-noise, stressing this point, will be discussed elsewhere). These features corroborate the idea of a maximum of 'complexity' during the transition in terms of shapes dynamics. Since the very meaning of complexity is often difficult to establish, a regular presence of the phenomena we are discussing could be used, in unknown dynamical processes, to define, test or characterize their complexity.

6. Conclusion

In conclusion, checks confirm the reliability of the approach based on rational partitions, in the particular form we have introduced here, to study the appearance of complex phenomena in two-dimensional discrete models.

References

[1] Casartelli M 1990 *Complex Syst.* **4** 491–507
[2] Albrigi A and Casartelli M 1993 *Complex Syst.* **7** 171–97
[3] Peierls R 1936 *Proc. Cambridge Phil. Soc.* **32** 477
[4] Griffiths R B 1964 *Phys. Rev.* A **136** 437
[5] Derrida B and Pomeau Y 1986 *Europhys. Lett.* **1** 45–52
[6] Grassberger P 1986 *Int. J. Theor. Phys.* **25** 907–38
[7] Binney J J, Dowrick N J, Fisher A J and Newman M E J 1993 *The Theory of Critical Phenomena* (New York: Oxford University Press)
[8] Kadanoff L P 1993 *From Order to Chaos* (Singapore: World Scientific)
[9] Solé R V and Luque B 1995 *Phys. Lett.* A **196** 331–4
[10] Solé R V, Manrubia S C, Luque B, Delgado J and Bascompte J 1995–6 *Complexity* **1** 13–26
[11] Badii R and Politi A 1997 *Complexity: Hierarchical Structure and Scaling in Physics* (Cambridge: Cambridge University Press)
[12] Vichniac G 1984 *Physica* D **10** 96–115
[13] Creutz M 1986 *Ann. Phys.* **167** 62–76
[14] Toffoli T and Margolus N 1987 *Cellular Automata Machines* (Cambridge, MA: MIT Press)